Semi-Poisson statistics in quantum chaos

Antonio M. García-García
Physics Department, Princeton University, Princeton, New Jersey 08544, USA
and The Abdus Salam International Centre for Theoretical Physics, P.O.B. 586, 34100 Trieste, Italy

Jiao Wang
Temasek Laboratories, National University of Singapore, 119260 Singapore
(Received 11 November 2005; published 14 March 2006)

We investigate the quantum properties of a nonrandom Hamiltonian with a steplike singularity. It is shown that the eigenfunctions are multifractals and, in a certain range of parameters, the level statistics is described exactly by semi-Poisson statistics (SP) typical of pseudointegrable systems. It is also shown that our results are universal, namely, they depend exclusively on the presence of the steplike singularity and are not modified by smooth perturbations of the potential or the addition of a magnetic flux. Although the quantum properties of our system are similar to those of a disordered conductor at the Anderson transition, we report important quantitative differences in both the level statistics and the multifractal dimensions controlling the transition. Finally, the study of quantum transport properties suggests that the classical singularity induces quantum anomalous diffusion. We discuss how these findings may be experimentally corroborated by using ultracold atoms techniques.

DOI: 10.1103/PhysRevE.73.036210 PACS number(s): 05.45.Mt, 05.40.−a, 71.30.+h, 72.15.Rn

I. INTRODUCTION

It is by now well established that the analysis of the level statistics is one of the main tools in the study of quantum complex systems. Moreover, the spectrum, unlike the wave functions, is easily accessible either numerically or experimentally. Part of this interest stems from the fact that, once the model-dependent spectral density is extracted from the spectrum, the level correlations of apparently unrelated models show striking universal features in a variety of physical situations. For instance, the celebrated Bohigas-Giannoni-Schmit conjecture (BGS) [1] states the level statistics of a quantum system whose classical counterpart is deterministic but fully chaotic does not depend on the microscopic details of the Hamiltonian but only on the global symmetries of the system and coincides with those of a random matrix with the same symmetry (usually referred to as Wigner-Dyson statistics (WD) [2]).

Remarkably, the same WD also describes [3] the spectral correlations of a disordered system [4] in the metallic limit. By contrast, for disorder strong enough, eigenstates localization becomes important, the spectrum is not correlated, and the level statistics is universally described by Poisson statistics. For deterministic systems Poisson statistics appears, provided that the classical dynamics is integrable [5].

Despite its robustness, the universality associated with WD also has clear limits of applicability. For instance, the quantum properties of Hamiltonians whose classical phase space is a superposition of chaotic and integrable parts are supposed to depend dramatically on the details of the Hamiltonian, and consequently their properties are nonuniversal. Similarly, for finite disordered systems in the metallic regime, the dimensionless conductance $g=E_c/\Delta$ (E_c, the Thouless energy, is a scale of energy associated with the classical diffusion time through sample and Δ is the mean level spacing) sets the number of eigenvalues whose spectral correlations are universally described by WD.

Universality in the spectral correlations also has a counterpart in the eigenfunctions properties. Thus, Poisson statistics is associated with exponential localization of the eigenfunctions, and WD is typical of systems in which the eigenstates are delocalized through the sample and can be effectively represented by a superposition of plane waves with random phases.

Recently, it was reported [6–8] that the quantum properties of a disordered conductor at the metal-insulator transition [usually referred to as the Anderson transition (AT)] are to a certain extent also universal. Features related to this new universality class include multifractal eigenstates [9] and level statistics given by critical statistics [7] (see below for a definition). Intuitively [10] multifractality means that eigenstates have structures at all scales. Roughly speaking, the amplitude of probability of a multifractal eigenstate has peaks ("probability splashes") at all scales decaying as a power law from its maximum. Consider the volume of the subset of a box for which the absolute value of the wave function Ψ is larger than a fixed number M. If this volume scales as L^{d^*} (with $d^*<d$), then d^* is called the fractal dimension of Ψ. In case the fractal dimension depends on the value of M, the wave function is said to be multifractal. On a more formal level multifractality is defined either through the box counting method (see [25] and Sec. III C below) or the anomalous scaling of the eigenfunction moments $\mathcal{P}_q=\int d^dr|\psi(\mathbf{r})|^{2q}$ with respect to the sample size L as $\mathcal{P}_q \propto L^{-D_q(q-1)}$, where D_q is a set of exponents describing the AT [9]. "Critical statistics" [6,7] (the level statistics at the AT) is intermediate between Wigner-Dyson and Poisson statistics. Typical features include: scale invariant spectrum [6], level repulsion, and asymptotically linear number variance [8].

Level and eigenfunction correlations at the AT are said to be universal in the sense that typical features of critical statistics as level repulsion, scale invariance, and linear number

variance $[\Sigma^2(L)=\langle L^2\rangle-\langle L\rangle^2=\chi L$ for $\chi<1$ and $L\gg 1]$ do not depend on boundary conditions, the shape of the system, or the microscopic details of the disordered potential [11]. However, the slope of the number variance or the functional form of certain level correlators as the level spacing distribution $P(s)$ (the probability of having two eigenvalues at a distance s) may depend on additional parameters as the dimensionality of the space.

Another argument reinforcing the universality of critical statistics is the fact that, as for WD, which describes the level statistics of a Gaussian random matrix model, critical statistics has also been found in a variety of generalized random matrix models: based on soft confining potentials [12], effective eigenvalue distributions [13,14] related to the Calogero-Sutherland model at finite temperature, and random banded matrices with power-law decay [15]. The latter is especially interesting since an AT has been analytically established by mapping the problem onto a nonlinear σ model.

Finally, we recall that critical statistics is not related to any ergodic limit of the quantum motion as in the case of WD. Consequently, it is capable to describes nontrivial dynamical features and its limit of validity is not restricted to a scale given by the dimensionless conductance g (as for WD).

A natural question to ask is whether critical statistical and multifractal wave functions are exclusive of disordered systems or may also appear in deterministic quantum systems. Indeed, in a recent Letter [16] we have established a relation between the presence of anomalous diffusion in the classical dynamics, the singularities of a classically chaotic potential, and the power-law localization of the quantum eigenstates. Specifically, for a certain kind of singularity (log for 1+1D system) associated with classical $1/f$ noise, it is found that the level statistics is described by critical statistics and the eigenstates are multifractal with a D_q quantitatively similar to the one at the AT. These results are universal in the sense that neither the classical nor the quantum properties depend on the details of the potential but only on the type of singularity.

Other nonrandom systems whose level statistics has been reported to be similar to critical statistics include: Coulomb billiards [17], anisotropic Kepler problem [18], generalized kicked rotors [19], and pseudointegrable billiards [20,21]. For the latter the dynamics is intermediate between chaotic and integrable and, in order to fit the spectrum, Bogomolny and co-workers introduced [20] a purely phenomenological short-range plasma model whose joint distribution of eigenvalues [20] is given by the classical Dyson gas with the logarithmic pairwise interaction restricted to a finite number k of nearest neighbors. Explicit analytical solutions are available for general k. For instance, for $k=2$ (usually referred to as semi-Poisson statistics SP), $R_2(s)=1-e^{-4s}$, $P(s)=4se^{-2s}$, and $\Sigma^2(L)=L/2+(1-e^{-4L})/8$, where $R_2(s)$ is the two-level correlation function (TLCF). In passing, we mention that SP can also be obtained by removing every k eigenvalue out of a spectrum with Poisson statistics. It turns out that this short-range plasma model reproduces typical characteristics of critical statistics such as level repulsion and linear number variance with a slope depending on k.

However, SP is quantitatively different from critical statistics. In critical statistics, as mentioned above, the joint distribution of eigenvalues can be considered as an ensemble of free particles at finite temperature with a nontrivial statistical interaction. The statistical interaction resembles the Vandermonde determinant, and the effect of a finite temperature is to suppress the correlations of distant eigenvalues. In the case of SP this suppression is abrupt [20] since only nearest-neighbor levels can interact. Thus, critical statistics and SP share similar generic features but are in principle quantitatively different.

The aim of this paper is to establish under what generic circumstances one may expect SP in the context of nonrandom Hamiltonians.

For the sake of clearness we enunciate our main conclusions: We have found that the appearance of SP can indeed be traced back to the presence of a certain kind of singularity (different from the one associated with critical statistics) in the classical potential. It is shown that SP is indeed robust under arbitrary smooth perturbations of the classical potential or the insertion of a magnetic flux provided that the classical singularity is preserved. The eigenfunctions associated with SP are found to be multifractal but quantitatively different from those of a disordered conductor at the AT. Finally, we argue that quantum anomalous diffusion induced by the classical singularity may be verified experimentally by using ultracold atoms techniques.

The organization of the paper is as follows. In the next section we introduce the model: a generalized kicked rotor in a potential with a steplike singularity. In Sec. III we discuss analytical results available for our model, then we investigate the level statistics and perform a multifractal analysis of the eigenstates. Finally, in Sec. IV we examine the quantum diffusion of our model and discuss possible ways of experimental verification.

II. THE MODEL

We investigate a generalized kicked rotor in 1+1D with a steplike singularity,

$$\mathcal{H}=\frac{p^2}{2}+V(q)\sum_n \delta(t-nT), \tag{1}$$

with $q\in[-\pi,\pi)$, where $V(q)$ is an arbitrary nonanalytical function with a steplike singularity. The simplest case corresponds to

$$V(q)=\begin{cases} v_0, & \text{if } q\in[-a,a) \\ 0, & \text{otherwise,}\end{cases} \tag{2}$$

where a sets the size of the step and v_0 the height. We shall see in a broad range of parameters our results do not depend on the specific form of $V(q)$ but only on the presence of the singularity.

The quantum dynamics is governed by the quantum evolution operator $\mathcal{U}$ over a period T. Thus, after a period T, an initial state ψ_0 evolves to $\psi(T)=\mathcal{U}\psi_0=e^{-i\hat{p}^2T/4\bar{h}}e^{-iV(\hat{q})/\bar{h}}e^{-i\hat{p}^2T/4\bar{h}}\psi_0$, where $\hat{p}$ and $\hat{q}$ stand for the usual momentum and position operator. Our aim is to solve the eigenvalue problem $\mathcal{U}\Psi_n=e^{-i\kappa_n/\hbar}\Psi_n$, where Ψ_n is an

eigenstate of $\mathcal{U}$ with quasieigenenergy κ_n. In order to proceed, we first express the evolution operator $\langle m|\mathcal{U}|n\rangle = U_{nm}$ in a basis of momentum eigenstates $\{|n\rangle = (e^{in\theta}/2\pi)\}$ with $n=0,\ldots,N\to\infty$,

$$U_{mn} = \frac{e^{-i(T\hbar/4)(m^2+n^2)}}{2\pi}\int_{-\pi}^{\pi} dq e^{iq(m-n)-iV(q)/\hbar} \tag{3}$$

We remark that in this representation, referred to as "cylinder representation," the resulting matrix U_{nm} is unitary exclusively in the $N\to\infty$ limit. For practical calculations this is certainly a disadvantage since, besides typical finite size, one also has to face truncation effects, namely, the integral of the density of probability is not exactly the unity and eigenvalues are not pure phases $(e^{-i\theta_n})$ as expected in a unitary matrix.

An alternative procedure, referred to as "torus representation," especially suited for numerical calculations, is to make the Hilbert space finite (i.e., $m,n=1,\ldots,N$) but still keep the matrix unitary. This can be achieved by imposing periodicity (with period $P\sim N$) in momentum space. With these choices $\hbar$ is set to the unity since the period in momentum $P\sim N$ and the period in position $Q\sim 2\pi$ are related by $PQ=2\pi N\hbar$. Thus, the period on momentum is large $(P=N)$ and the phase space effectively resembles a cylinder (for more details see [22]).

In order to keep the kinetic term of the evolution matrix also periodic, we take $T=2\pi M/N$ with M an integer (not a divisor of N). For technical reasons (see below) M is chosen to make T roughly constant (≈ 0.1 in this paper) such that M/N is a good approximation to an irrational for every N used. The resulting evolution matrix (for N odd) then reads

$$\langle m|\mathcal{U}|n\rangle = \frac{1}{N}e^{-i(\pi M/2N)(m^2+n^2)}\sum_l e^{i\phi(l,m,n)}, \tag{4}$$

where $\phi(l,m,n)=2\pi(l+\theta_0)(m-n)/N - V(2\pi(l+\theta_0)/N)$, $l=-(N-1)/2,\ldots,(N-1)/2$ and $0\leqslant\theta_0\leqslant 1$; θ_0 is a parameter depending on the boundary conditions ($\theta_0=0$ for periodic boundary conditions).

In this paper we shall use both representations depending on the issue to be discussed. Thus, for the analytical analysis the cylinder representation is more appropriate: the limit $N\to\infty$ can be effectively taken and consequently truncation effects are absent. For the numerical calculations we use the torus representation due to the difficulty to deal with truncation effects. An exception is the case of quantum diffusion, where these effects can be accurately detected and subtracted from the calculation. As a final remark we mention that the numerical evaluation of the eigenvalues and eigenvectors of $\mathcal{U}$ (either for the torus or the cylinder) is carried out by using standard diagonalization techniques for volumes ranging from $N=500$ to $N=8000$. For $\theta_0=0$, parity is a good quantum number and consequently states with different parity must be treated separately.

III. RESULTS

For the sake of clearness we first summarize our main results:

(1) The level statistics associated with the evolution matrix of the Hamiltonian Eq. (1) is scale invariant and given by SP in the region $S=\tan(v_0/2)\gg 1$, where v_0 is the height of the steplike potential. These results are universal: they neither depend on the specific form of $V(q)$ (provided that the singularity is preserved) nor on any source (as a magnetic flux) of time-reversal symmetry.

(2) In the limit $S=\tan(v_0/2)\ll 1$ the spectrum is scale invariant and well described by Poisson statistics. For intermediate values of S we observe a transition from SP to Poisson as S is decreased.

(3) In the SP region the eigenstates are multifractal but with a multifractal spectrum $D_q\sim A/q+D_\infty$ essentially different from the one observed at the AT.

(4) The classical singularity induces quantum anomalous diffusion.

A. Analytical results

In this section we investigate what kind of analytical information can be obtained from the Hamiltonian Eq. (1). Our aim is to show that in a certain range of parameter the level statistics associated with Eq. (1) is exactly given by SP. In a first step we map, following the standard prescription of Ref. [23], the evolution matrix Eq. (4) onto a 1D Anderson model. For smooth potentials such mapping results in a standard 1D Anderson model with short-range hopping. As known, for this kind of model eigenstates are exponentially localized for any amount of disorder and consequently dynamical localization has been reported [23] in the associated kicked-rotor system.

However, in our case the situation is different. The classical steplike singularity induces long-range correlations in the associated 1D Anderson model,

$$\mathcal{H}\psi_n = \epsilon_n\psi_n + \sum_m F(m-n)\psi_m, \tag{5}$$

where $\epsilon_n\sim\tan(Tn^2)$,

$$F(m-n) = \int_{-\pi}^{-\pi} d\theta \tan[V(\theta)/2]e^{-i\theta(m-n)} = A\frac{\sin\gamma(m-n)}{m-n},$$

$A\sim\tan(v_0/2)$, and $\gamma=a$. For ϵ_n, a random number from a box distribution $[-W/2,W2]$, it has been shown recently [24] (see the discussion below) without invoking any ensemble average that the level statistics is exactly given by SP in the limit $A\gg W$. However, as A gets comparable to W a shift to Poisson is observed. Thus, for our Hamiltonian Eq. (1) the region in which SP holds corresponds with $v_0\sim\pi$ $[A=\tan(v_0/2)\gg 1]$. Moreover, T must be such that $\epsilon_n\sim\tan(Tn^2)$ is approximately random; this always occurs for $T\sim 1$ irrational. In the torus representation of the evolution matrix T must be rational so in order to overcome this problem we set T to be a good approximation to an irrational number.

For the sake of completeness the rest of this section is devoted, following Ref. [24], to a technical account of the reasons for the appearance of SP in the Hamiltonian Eq. (5). We recall that throughout the demonstration the diagonal en-

ergy ϵ_n is assumed to be strictly random. First, we express the Hamiltonian (5) in Fourier space as

$$\mathcal{H} = E_k \psi_k + \sum_{k \neq k'} \hat{A}(k,k') \psi'_k,$$

where

$$E_k = \sum_r \frac{\sin \gamma r}{r} e^{ikr}$$

and

$$\hat{A}(k,k') = \frac{1}{N} \sum_n \epsilon_n e^{-in(k-k')}.$$

We set $\gamma = \pi/2$ (our findings do not depend on γ). After a simple calculation we find that E_k is not a smooth function (this steplike singularity is indeed the seed for the appearance of SP); $E_k = A\pi/2$ for $k < \pi$ and $E_k = -A\pi/2$ for $k > \pi$. There are thus only two possible values of the energy separated by a gap $\delta = A\pi$. Upon adding a weak ($A \gg W$) disordered potential this degeneracy is lifted and the spectrum is composed of two separate bands of size $\sim W$ around each of the bare points $-A\pi/2, A\pi/2$. Since the Hamiltonian is invariant under the transformation $A \to -A$, the spectrum must also possess that symmetry. That means that, to leading order in A (neglecting $1/A$ corrections), the number of independent eigenvalues of Eq. (5) is $n/2$ instead of n.

We now show how this degeneracy affects the roots (eigenvalues) of the characteristic polynomial $P(t) = \det(H - tI)$. Let

$$P_{dis}(t) = a_0 + a_1 t + \cdots a_n t^n$$

be the characteristic polynomial associated with the disordered part of the Hamiltonian. We remark that, despite its complicated form, its roots by definition are random numbers with a box distribution $[-W, W]$. On the other hand, in the clean case,

$$P_{clean}(t) = (t - A)^{n/2} (t + A)^{n/2}$$

(π factors are not considered). Due to the $A \to -A$ symmetry, the full [Eq. (5)] case P_{full} corresponds with P_{dis} but replacing t^k factors by a combination $(t-A)^{k_1}(t+A)^{k_2}$ with $k_1 + k_2 = k$. The roots of P_{full} will be in general complicated functions of A. However, in the limit of interest, $A \gg W \to \infty$, an analytical evaluation is possible. By setting $t = t_1 - A$ we look for roots t_1 of order of the unity in the A band. We next perform an expansion of the characteristic polynomial P_{full} to leading order in A. Thus, we keep the terms $A^{n/2}$ and neglect lower powers in A. The resulting P_{full} is given by

$$P_{full} = t_1^{n/2} + \frac{a_{n-2} t_1^{n/2-2}}{3} + \frac{a_{n-3} t_1^{n/2-3}}{4} + \cdots 2\frac{a_{n/2+1} t_1}{n} + 2\frac{a_{n/2}}{n+2},$$

where the coefficients a_n are the *same* as those of P_{dia} above but only $n/2$ of them appear in the full case. The eigenvalues ϵ'_i of Eq. (5) around the A band are $\epsilon'_i = A + \beta_i$, with β_i a root of P_{full}. The effect of the long-range interaction is just to remove all the terms with coefficients a_0 to $a_{n/2}$ from the characteristic polynomial of the diagonal disordered case.

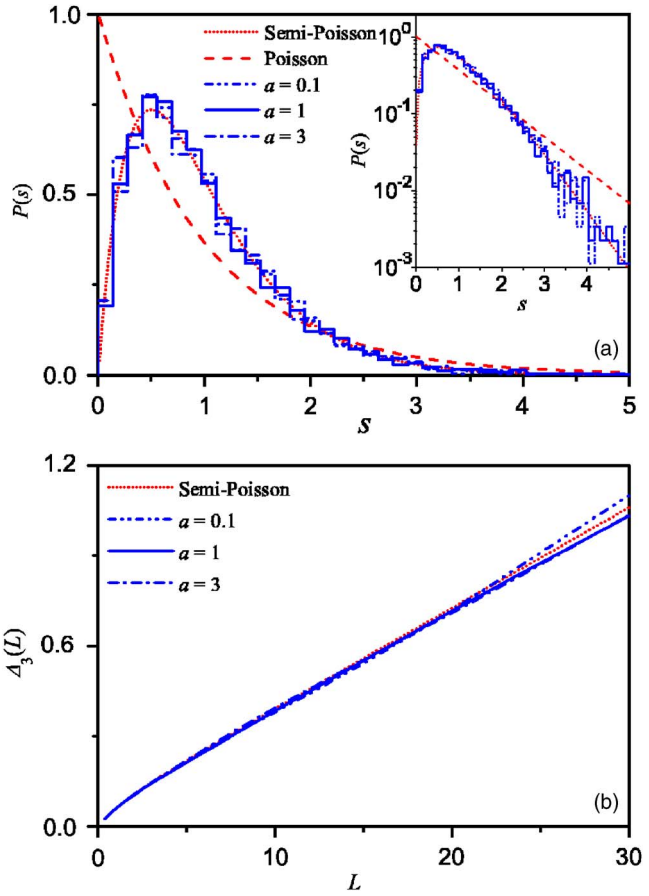

FIG. 1. (Color online) Level spacing distribution $P(s)$ (a) and spectral rigidity $\Delta_3(L)$ (b) for the spectrum of the evolution matrix Eq. (4) with potential Eq. (2) for different widths a and $v_0 = \pi$. In all cases the size of the evolution matrix is $N = 6397$. The agreement with SP is excellent.

The spectrum is thus that of a pure diagonal disorder where half of the eigenvalues have been removed. The remaining eigenvalues are still symmetrically distributed (the ones with largest modulus are well approximated by $t_{max} = \pm\sqrt{(a_{n-2})/3}$) around A. That means, by symmetry considerations, that the removed ones must be either the odd or the even ones. This is precisely the definition of semi-Poisson statistics. In conclusion, our model reproduces exactly the mechanism which is utilized in the very definition of SP. We finally mention that the only effect of the coefficients $3, 4 \ldots, n+2/2$ is to renormalize the effective size of the spectrum: $\sim 2W$ for diagonal disorder and $\sim 2W/\sqrt{3}$ for Eq. (5).

B. Level statistics

The above analytical arguments have been fully corroborated by numerical calculations. As mentioned previously, in order to avoid truncation effects we have chosen the torus representation of the evolution matrix. Our first goal is to show that the level statistics of our model with the potential of Eq. (2) is given by SP in the region $S = \tan(v_0/2) \gg 1$ for any a. In Fig. 1 we plot the level spacing distribution $P(s)$ for different values of a and $S \gg 1$. As observed, the agree-

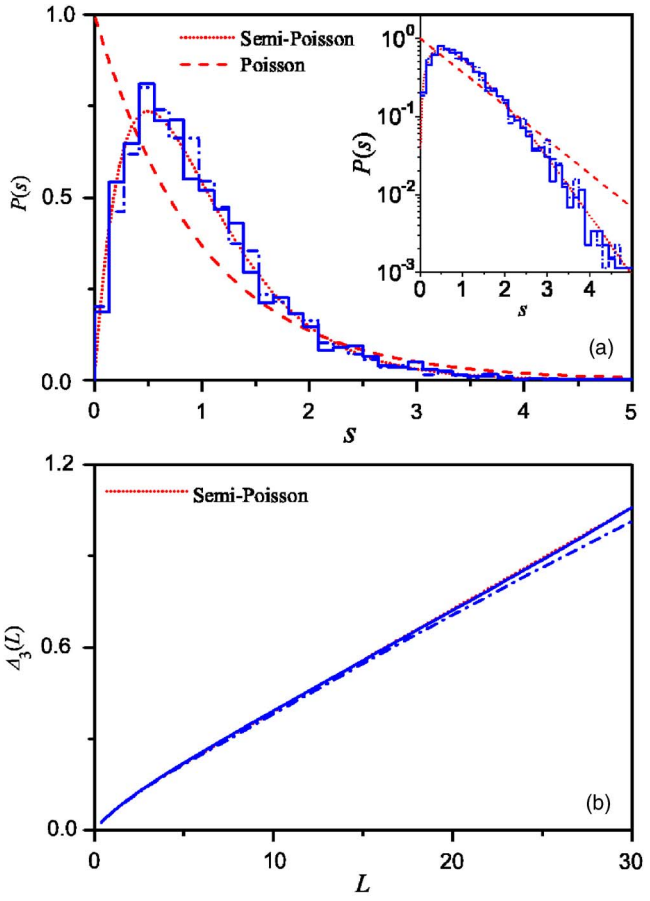

FIG. 2. (Color online) Level spacing distribution $P(s)$ (a) and spectral rigidity $\Delta_3(L)$ (b) of the spectrum of the evolution matrix ($N=6397$) Eq. (4) with potential Eq. (2) and $v_0=\pi$ and $a=\pi/2$. As observed, the level statistics is not affected either by the breaking of the time-reversal invariance (dashed-dotted) line or by the addition of a smooth perturbation (solid line) $V_{per}=c_1\cos(q)+c_2\sin(q)+c_3\cos(2q)+c_4\sin(2q)$ with random c_i (see the text).

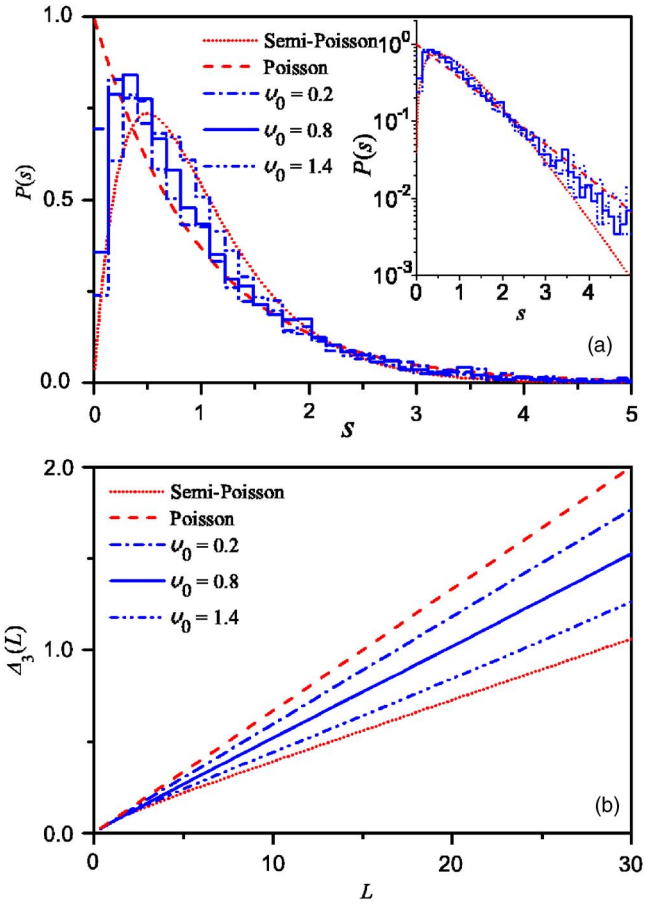

FIG. 3. (Color online) Level spacing distribution (a) and spectral rigidity (b) of the evolution matrix ($N=6397$) Eq. (4) for the potential Eq. (2) for different v_0 and $a=1$. A transition from SP to Poisson is found as v_0 goes from π to 0.

ment with SP is excellent in all cases even in the tail of the distribution and it is not restricted to short-range correlators. As shown in Fig. 1(b), the study of long-range correlators as the spectral rigidity $\Delta_3(L)=(2L^4)\int_0^L(L^3-2L^2r+r^3)\Sigma^2(r)dr$ further confirms this point. Up to scales of 30–40 eigenvalues deviations from SP are almost indistinguishable for different values of the parameters. Deviations for larger scales are due to well-known finite size effects. Although not shown, we have also checked that in the range of volumes accessible to numerical techniques, the level statistics was to a great extent scale invariant, namely, it was independent from the system size. Once the region in which SP holds has been established, we investigate the robustness and universality of these results. In order to proceed we have repeated the level statistics analysis for a potential with a nonanalytical steplike form but perturbed by a smooth chaotic potential. As shown in Fig. 2, neither short- nor long-range spectral correlators are affected by the chaotic perturbation provided that the steplike nonanalyticity is preserved. The perturbation potential V_{per} used in Fig. 2 is defined by $V_{per}=c_1\cos(q)+c_2\sin(q)+c_3\cos(2q)+c_4\sin(2q)$, with c_i randomly chosen from a uniform distribution (0, 1). We have also checked that higher frequency components $\sim\cos(3q)$ do not change the results provided that $|V_{pert}|\ll v_0$.

In addition, we have found that the level statistics is not modified if time-reversal invariance is broken by adding a magnetic flux to Eq. (1) (which is equivalent to setting T as an irrational multiple of 2π; see [16]). These results indicate that SP is universal; namely, it does not depend on the details of the potential provided that the steplike singularity is still present.

Finally, we study the transition to Poisson statistics as the parameter $S=\tan(v_0/2)$ goes from $S\gg 1$ (SP region) to $S\ll 1$. As shown in Fig. 3 the level statistics [both $P(s)$ and $\Delta_3(L)$] seems to move smoothly from SP to Poisson. All of the typical features of criticality mentioned above are maintained through the transition. Of course, parameters as the slope of the number variance χ run from $\chi=1/2$ (SP) to $\chi=1$ (Poisson) as S is decreased. However, we stress that, unlike the SP region, it is hard to define unambiguously a universality class in the transition region. The point is that, in essence, the appearance of SP can be traced back (see analytical results) to the gap in the spectrum of the Hamiltonian. The steplike singularity thus separates the spectrum in two different bands around the only two eigenvalues in the clean case. As the disorder strength becomes comparable with the

numerical value of the bare eigenvalues, both bands mix up and the spectrum deviates from SP. We could not find any sign of universality in the way in which this mixing occurs since it may depend on the microscopic details of the potential. Due to this lack of universality, in the rest of the paper we will focus our investigation mainly on the region of parameters associated with SP.

C. Eigenvector analysis

We now investigate the eigenvector properties of the Hamiltonian Eq. (1) with potential Eq. (2) in the region $S \gg 1$ corresponding to SP.

This choice stems from the fact that, as shown above, the quantum properties do not depend on the details $V(q)$ but only on the presence of the steplike singularity. For the numerical calculation we have again utilized the torus representation of the evolution matrix in order to avoid leaking of probability due to truncation effects.

We have two clear objectives in this section. On the one hand we would like to investigate whether the eigenvectors associated with SP are multifractal as at the AT. Once this question is answered affirmatively our intention is to provide a careful and detailed analysis of the anomalous dimension D_q controlling the eigenstate's multifractality. Based on the numerical findings we conjecture the relation $D_q = A/q + D_\infty$, which we claim to be valid for all systems with SP. To start, we give a detailed account on how D_q was computed. We use the standard box-counting procedure [25]. In doing so, for a given eigenvector $\psi = \Sigma_{k=1}^{N} \psi_k |k\rangle$ of the system we first distribute all the components into $N_l = N/l$ boxes of the same size l, then associate a probability $p_i = \Sigma_k |\psi_k|^2$ with each box with $k \in [il, (i+1)l)$; $i = 1, \ldots, N_l$. The normalized qth moments of p_i define the generalized fractal dimensions [26],

$$D_q(N) = \frac{1}{q-1} \lim_{\delta \to 0} \frac{\ln \sum_{i=1}^{N_l} p_i^q}{\ln \delta}, \tag{6}$$

where $\delta = l/N$ is the size of the box normalized by the system size N. In practical calculations D_q is evaluated over an appropriate range of δ by performing a linear regression of $\log \Sigma_{i=1}^{N_l} p_i^q$ with $\ln \delta$ (usually $\alpha/N \leqslant \delta \leqslant 1/2$, where α is a characteristic microscopic length scale of the system [25]). In our case a good linear dependence of $\ln \Sigma_{i=1}^{N_l} p_i^q$ on $\ln \delta$ is observed in the region $\delta \in (0.022, 0.45)$ for a broad range of the potential parameters v_0, a of Eq. (2). $D_q(N)$ is thus computed by linear regression over this δ window for each eigenvector. Since $D_q(N)$ is a self-averaging [15] quantity, the mean value $\langle D_q(N) \rangle$ over all eigenstates provides a meaningful description of the multifractal properties of the system. We observe that, even after this averaging, the statistical fluctuations of $\langle D_q(N) \rangle$ are still quite strong. In order to minimize these fluctuations we perform an additional average over realizations of the evolution operator Eq. (4) until we obtain around 36 000 eigenvalues for each value of N (see Fig. 4). We generate different realizations of the evolution matrix by varying the period T. In the time-reversal invariant case ($T = 2\pi M/N$) this is done by picking up different values of M, and in the broken time-reversal case ($T = 2\pi\beta$ with β irrational) by choosing different values of β.

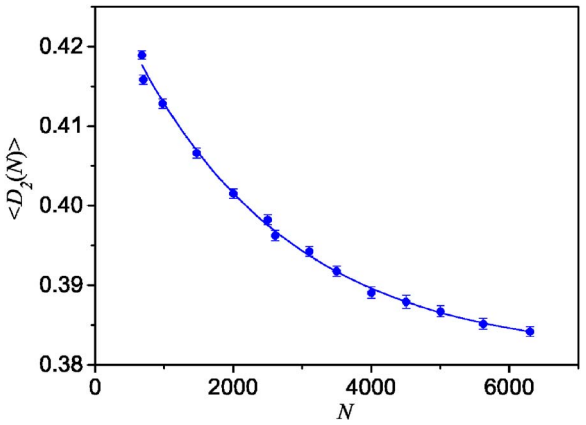

FIG. 4. (Color online) System size dependence of the multifractal dimension $\langle D_2(N) \rangle$. For each N the average is taken over around 36 000 eigenstates of the evolution operator Eq. (4) with the potential given by Eq. (2) and $a = 1$, $v_0 = \pi$. The best-fitting function is a exponential $(0.0493 \pm 0.0007) e^{-N/(2290 \pm 122)} + D_2$ with $D_2 = 0.381 \pm 0.001$ (solid curve).

As observed in Fig. 4, the $\langle D_q(N) \rangle$ thus obtained has a significant dependence on the system size which gets smaller as we approach the thermodynamic limit. In order to remove this finite size effect from $\langle D_q(N) \rangle$ we have tried different fittings, $\langle D_q(N) \rangle = D_q + f(N, a, b)$ with $f(N, a, b) \to 0$ as $N \to \infty$ and a, b, D_q fitting parameters. Thus, the parameter D_q corresponds with the $N \to \infty$ limit of $\langle D_q(N) \rangle$. We found that for various values of q the choice of f that best describes the finite size corrections is $f(N, a, b) = a e^{-N/b}$ (see Fig. 4 for the case $q = 2$).

After the technical analysis we are ready to present our results. First, we have found that the eigenstates are indeed multifractal. As shown in Fig. 5, D_q [the $N \to \infty$ of $\langle D_q(N) \rangle$] depends clearly on q. We have also found that D_q is very robust. Thus, it is not affected by different choices of a, $v_0 \sim \pi$, smooth perturbations to the potential Eq. (2), or by the breaking of the original time-reversal symmetry.

The next task we face is try to find an explicit expression for D_q. Unfortunately, we are not aware of any analytical technique capable of obtaining D_q exactly. The comparatively short range of q values for which numerical calculations are available, together with the statistical fluctuations, makes a numerical fitting ambiguous in the sense that many different fittings may yield quite satisfactory results. On the other hand, we think it is extremely important to have a proper characterization of D_q in order to completely define the universality class associated with SP. We found that the simplest expression for D_q still compatible with the numerical analysis is $D_q = A/q + D_\infty$ (with $A \sim 0.28$, and $D_\infty \sim 0.25$). As shown in Fig. 5 the agreement with the numerical results is very good. Remarkably, we have obtained a similar D_q in the study of the quantum evolution matrix associated with certain classical interval-exchange maps whose level statistics is exactly given by SP [21]. Based on this finding, we suggest that the D_q above describes the multifractal properties of all systems with SP.

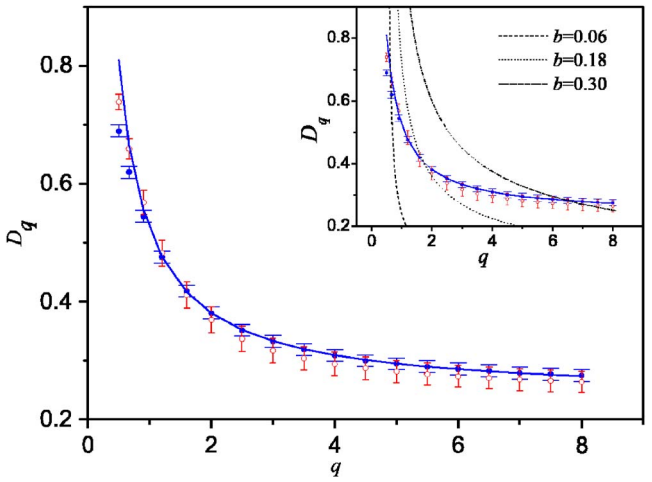

FIG. 5. (Color online) Generalized fractal dimensions D_q for the eigenvectors of the evolution matrix Eq. (4) with potential Eq. (2) and $a=1$, $v_0=\pi$. Solid dots are the results from Eq. (6) and the open dots are those obtained from the scaling of the averaged $\ln \mathcal{P}_q$ with $\ln N$ (see the text). The solid curve is the conjecture $A/q+D_\infty$, with $A=0.286\pm0.001$ and $D_\infty=0.238\pm0.001$. Inset shows the same results together with the prediction of critical statistics Eq. (7) for $b=0.06$, 0.18, and 0.30, respectively.

As a double check we have also evaluated D_q via the scaling of eigenfunction moments $\mathcal{P}_q=\int d^d r|\psi(\mathbf{r})|^{2q} \propto L^{-D_q(q-1)}$ with respect to the sample size $L=N$. In particular, D_q was obtained by linear regression of $\langle \ln \mathcal{P}_q \rangle$ with respect to $\ln N$. As in the previous case, the average is taken over all eigenvectors and different realizations of the evolution and finite size effects are removed by an appropriate fitting. The D_q obtained in this way is in complete agreement with the previous one within the numerical errors.

Finally, we compare the above D_q with the predictions of critical statistics. First, we remark that a comparison with a 3D (or 4D) disordered conductor at the AT is not entirely satisfactory since parameters as the slope of the number variance ($\sim$0.27 in the 3D case) defining the AT are different from the SP prediction (1/2). We thus find it more appropriate to compare the SP results with those of a random banded matrix with a power-law ($\sim 1/r$) decay and bandwidth b [15], where the spectral statistics is given by critical statistics and the multifractal character of the eigenstates has been established analytically. In the limit $b \ll 1$, closer to SP, it is found that for $q>1/2$

$$D_q = \frac{4b}{\sqrt{\pi}} \frac{\Gamma(q-1/2)}{\Gamma(q)}. \tag{7}$$

As shown in Fig. 5 (inset), this function does not describe the multifractal dimensions associated with SP for any b. Thus, we can conclude that despite their similarities critical statistics and SP belong to a different universality class.

IV. QUANTUM ANOMALOUS DIFFUSION AND EXPERIMENTAL VERIFICATION

In this section we investigate how quantum transport properties are affected by the steplike nonanalytical potential. Our motivation is twofold: On the one hand we wish to examine possible ways to test our results experimentally. On the other hand we are interested in finding out to what degree the phenomenon of dynamical localization typical of kicked rotors with smooth potentials $\sim\cos(q)$ is affected by the classical singularity. We recall that dynamical localization for smooth chaotic potentials manifests itself in the quantum suppression of classical diffusion in momentum space due to interference effects. Thus, contrary to the BGS conjecture [1], though the classical dynamics is chaotic, eigenstates are exponentially localized in momentum space and the level statistics is Poisson.

We start by computing both the quantum and classical density of probability $P(k,t)=|\langle k|\phi(t)\rangle|^2$ of finding a particle with momentum $p=k\hbar$ at time t for a given initial state $|\phi(0)\rangle=|0\rangle$ (initial condition in the classical case).

The first problem we face is that the potential Eq. (2) has a quite peculiar classical limit. The force exerted on the particle is a sum of two Dirac delta functions $\delta(q\pm a)$, namely, it vanishes elsewhere except at $q=\pm a$, where formally it diverges. Consequently, the classical motion is that of a free particle in a ring except for $q=\pm a$, where it gets an infinite force. Obviously, in order to compare classical with quantum predictions one first has to smooth the step potential. Thus, for the analysis of dynamical localization we consider the potential

$$V(q) = Si[(a+q)/\sigma] + Si[(a-q)/\sigma], \tag{8}$$

where $Si(q)=\int_0^q[\sin(t)t]dt$ is the sine integral function. For $\sigma \to 0$ we recover the steplike potential. The classical force associated with this potential is $F(q)=[1/(a-q)]\sin[(a-q)/\sigma]-[1/(a+q)]\sin[(a+q)/\sigma]$ (Dirac delta functions in the limit $\sigma \to 0$). With this potential we get a well-defined classical limit for any finite σ. We have computed the classical $P(p,t)$ by evolving the classical equation of motion for 10^6 different random initial conditions with zero momentum $p=0$ and uniformly distributed position along the interval $(-\pi,\pi)$. We have found that $P(p,t)\sim 2Dt/p^2$ for $|p|<c(\sigma)\sqrt{2Dt}$, where $D\sim 1/2\sigma$ and $c(\sigma)$ increases as σ decreases. Outside this region $P(p,t)$ resembles that of a standard diffusion process. Thus, for sufficiently small p and t the diffusion is anomalous and then gradually becomes normal. In Fig. 6 we plot the quantum and classical variance $\langle p^2(t)\rangle$ of the density of probability $P(p,t)$ ($p=\hbar k$ for the quantum case) measured at time t. Calculations were carried out for the differentiable potential of Eq. (8). It is observed that, as expected, for short times both classical and quantum results coincide. However, after a certain breaking time $t_b \propto D \approx 100$ the quantum particle still diffuses but at a slower rate than the classical one, thus suggesting that diffusion is weakened by quantum interference effects. We relate this new region of weak dynamical localization to the effect of the classical singularity on the quantum dynamics.

For even longer times $t_c \sim 20\,000$ related to the crossover to normal classical diffusion the quantum particle tends to localize in momentum space as a consequence of standard dynamical localization effects. The latter regime is due to the underlying smooth nature of the potential investigated. Thus,

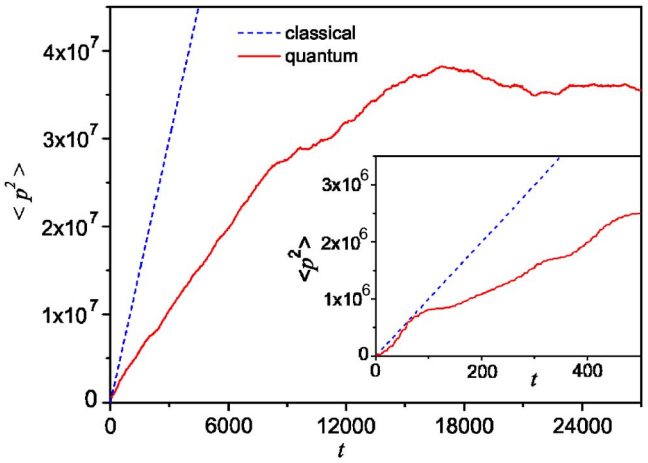

FIG. 6. (Color online) Classical and quantum variance $\langle p^2(t)\rangle$ of the density of probability $P(p,t)$ (see the text) for the Hamiltonian Eq. (1) ($T=1$, $\hbar=1$) and potential given by Eq. (8) with $\sigma=10^{-4}$. The classical counterpart was obtained from 10^6 random initial conditions with zero initial momentum and uniformly distributed q in $(-\pi,\pi)$.

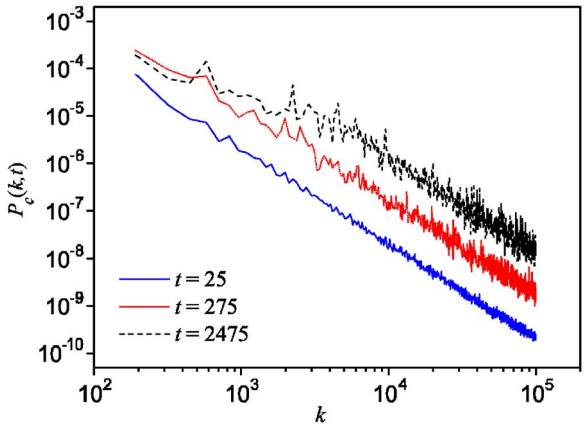

FIG. 7. (Color online) Quantum coarse-grained $P(k,t)$ versus k at various times t associated with the potential Eq. (2) ($v_0=\pi$ and $a=\pi/2$) plus a perturbation $V_{per}(q)=8\cos(q)$. For a given pair of k and t, $P_c(k,t)$ is the average of $P(k',t')$ over $k'=k-63,\ldots,k+64$ and $t'=t-24,\ldots,t+25$. $P_c(k,t)$ has power-law tails $\sim t^{0.84\pm0.01}|k|^{-2}$ for $|k|\gg t/\hbar\rho$, where ρ is the spectral density. Similar results are observed if only the potential Eq. (2) is considered.

in order to observe genuine quantum effects associated with classical singularities the value of σ must be such that $t_b \ll t_c$. We remark that this condition should be met by any experiment aiming to confirm the results reported in this paper.

For the sake of completeness we have also investigated the specific form of the quantum $P(k,t)$ as a function of k [from now on we switch back to our original potential Eq. (2)]. In the context of a disordered conductor it has been reported that [27] at the AT the quantum diffusion is anomalous. For time scales large enough the density of probability has a power-law form with the exponent depending on the multifractal dimension D_2. Similar results have also been obtained recently in momentum space for a kicked rotor with a logarithmic singularity [16]. As expected, we have also observed power-law tails in our model in both the short and the long t limit. For $|k|\gg t/\hbar\rho$ (with $\rho=1/2\pi$ the spectral density) a best-fit estimate yields $P(k,t)\sim t^{0.84\pm0.01}|k|^{-2}$ (see Fig. 7), similar to the classical prediction. By contrast, in the opposite limit though power-law tails have also been found the diffusion is slower, in agreement with previous findings.

Another feature induced by the steplike singularity is the power-law localization of the eigenstates. In Fig. 8 it is clearly observed that the eigenstates [28] have power-law tails with an exponent around minus 1. This is in clear contrast with the exponential localization observed in the kicked rotor with a smooth potential. However, it is similar to the case of a potential with a log singularity [16]; not surprisingly, in both cases the off-diagonal elements of the evolution operator present a similar power-law decay [15]. We mention that there is no contradiction between this smooth power-law behavior and the multifractal features investigated previously. The point is that the multifractal character of the eigenstates appears as strong fluctuations around the smooth power-law behavior above. Roughly speaking, we can say that smooth power-law localization is the precursor of multifractality.

Finally, we discuss how the findings of this paper may be tested experimentally. The first direct experimental realization of the quantum kicked rotor with a smooth potential was reported by Raizen [29] and co-workers in 1995. The experimental setup consisted of a dilute sample of ultracold atoms (typically cesium or sodium) "kicked" by a periodic standing wave of near-resonant light that is pulsed on periodically in time to approximate a series of delta functions. The typical output of the experiment is the distribution of the atom momentum as a function of time. It is also possible to estimate the quantum breaking time signaling the beginning of quantum localization. For the case of a smooth periodic standing wave, dynamical localization was also detected experimentally, in full agreement with the theoretical predictions. We thus propose that the full $P(k,t)$, the accumulated probability

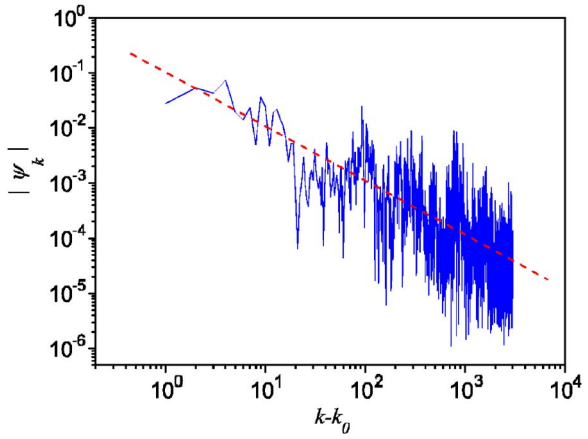

FIG. 8. (Color online) A typical eigenstate of the evolution matrix Eq. (4) ($T=1$, $\hbar=1$) with potential Eq. (2) ($v_0=\pi$ and $a=\pi/2$) plus a perturbation $V_{per}=8\cos q$. The modulus of the eigenstate $|\psi_k|$ decays from its peak k_0 as a power law with an exponent close to -1. Indeed, the best fit (dashed line) corresponds to a slope of -0.98.

or the variance represented in Fig. 6 may by accessible to experimental verification provided that the smooth periodic standing wave is replaced by the steplike wave studied in this paper. Obviously, from a experimental point of view the steplike singularity is only approximated. Typically, the experimental signal is composed of a limited number of Fourier components and consequently it is smooth on sufficiently small scales (as the potential discussed in connection with dynamical localization). However, as we have shown in the previous section, we expect our results to hold in these "almost" nonanalytical potential at least up to a certain time scale related to the underlying smoothness of the potential.

V. CONCLUSIONS

In this paper we have studied a kicked rotator with a nonanalytical steplike singularity. It has been identified as a region of parameters where the level statistics is exactly given by SP. These results are universal in the sense that they do not depend on the specific form of the potential but only on the presence of the classical singularity. The eigenfunctions have been shown to be multifractal but with a set of multifractal exponents D_q different from the prediction of critical statistics. We have also conjectured, based on the numerical analysis and the comparison to other models with SP, that all systems described by SP have the same form of D_q ($D_q = A/q + D_\infty$). Finally, we have studied transport properties. It has been found that, unlike the standard kicked rotor, dynamical localization slows down but does not stop quantum diffusion. We have also discussed the possibility of experimental verification of our findings by using ultracold atoms kicked by a standing wave with an approximated steplike form.

ACKNOWLEDGMENTS

A.M.G. acknowledges financial support from Marie Curie individual action program under Contract MOIF-CT-2005-007300. J.W. is supported by DSTA Singapore under Project Agreement No. POD0001821.

[1] O. Bohigas, M. J. Giannoni, and C. Schmit, Phys. Rev. Lett. **52**, 1 (1984).
[2] M. L. Mehta, *Random Matrices*, 2nd ed. (Academic Press, San Diego, 1991).
[3] K. B. Efetov, Adv. Phys. **32**, 53 (1983).
[4] P. W. Anderson, Phys. Rev. **109**, 1492 (1958).
[5] M. V. Berry and M. Tabor, Proc. R. Soc. London, Ser. A **356**, 375 (1977).
[6] B. I. Shklovskii, B. Shapiro, B. R. Sears, P. Lambrianides, and H. B. Shore, Phys. Rev. B **47**, 11487 (1993).
[7] V. E. Kravtsov and K. A. Muttalib, Phys. Rev. Lett. **79**, 1913 (1997); S. M. Nishigaki, Phys. Rev. E **59**, 2853 (1999).
[8] B. L. Altshuler, I. K. Zharekeshev, S. A. Kotochigova, and B. I. Shklovskii, Sov. Phys. JETP **67**, 62 (1988).
[9] H. Aoki, J. Phys. C **16**, L205 (1983).
[10] V. E. Kravtsov, e-print cond-mat/9603166.
[11] D. Braun, G. Montambaux, and M. Pascaud, Phys. Rev. Lett. **81**, 1062 (1998).
[12] K. A. Muttalib, Y. Chen, M. E. H. Ismail, and V. N. Nicopoulos, Phys. Rev. Lett. **71**, 471 (1993); Y. Chen and K. A. Muttalib, J. Phys.: Condens. Matter **6**, L293 (1994).
[13] M. Moshe, H. Neuberger, and B. Shapiro, Phys. Rev. Lett. **73**, 1497 (1994).
[14] A. M. García-García and J. J. M. Verbaarschot, Phys. Rev. E **67**, 046104 (2003).
[15] F. Evers and A. D. Mirlin, Phys. Rev. Lett. **84**, 3690 (2000); E. Cuevas, M. Ortuño, V. Gasparian, and A. Perez-Garido, *ibid.* **88**, 016401 (2001); A. D. Mirlin, Y. V. Fyodorov, F. M. Dittes, J. Quezada, and T. H. Seligman, Phys. Rev. E **54**, 3221 (1996).
[16] A. M. García-García and J. Wang, Phys. Rev. Lett. **94**, 244102 (2005).
[17] B. L. Altshuler and L. S. Levitov, Phys. Rep. **288**, 487 (1997).
[18] D. Wintgen and H. Marxer, Phys. Rev. Lett. **60**, 971 (1988).
[19] B. Hu, B. Li, J. Liu, and Y. Gu, Phys. Rev. Lett. **82**, 4224 (1999);J. Liu, W. T. Cheng, and C. G. Cheng, Commun. Theor. Phys. **33**, 15 (2000); C. E. Creffield, S. Fishman, and T. S. Monteiro, e-print physics/0510161; C. E. Creffield, G. Hur, and T. S. Monteiro, **96**, 024103 (2006).
[20] E. B. Bogomolny, U. Gerland, and C. Schmit, Phys. Rev. E **59**, R1315 (1999).
[21] E. Bogomolny and C. Schmit, Phys. Rev. Lett. **93**, 254102 (2004); O. Giraud, J. Marklof, and S. O'Keefe, J. Phys. A **37**, L303 (2004); E. Bogomolny and C. Schmit, Phys. Rev. Lett. **92**, 244102 (2004).
[22] F. M. Izrailev, Phys. Rep. **196**, 299 (1990).
[23] S. Fishman, D. R. Grempel, and R. E. Prange, Phys. Rev. Lett. **49**, 509 (1982).
[24] A. M. García-García, e-print cond-mat/0507272.
[25] M. Janssen, Int. J. Mod. Phys. B **8**, 943 (1994); B. Huckestein, Rev. Mod. Phys. **67**, 357 (1995); E. Cuevas, Phys. Rev. B **68**, 184206 (2003).
[26] H. G. E. Hentschel and I. Procaccia, Physica D **8**, 435 (1983).
[27] B. Huckestein and R. Klesse, Phys. Rev. B **59**, 9714 (1999).
[28] In the cylinder representation the eigenstates are obtained by diagonalizing a nonunitary truncated evolution operator. In order to evaluate the error involved in this approximation, we diagonalize both a truncated matrix of size N, $\mathcal{U}^{(N)}$, and a larger truncated matrix, say $\mathcal{U}^{(2N)}$, with $\mathcal{U}^{(N)}$ as its center. The truncation error is estimated to be $|(\mathcal{U}^{(2N)} - \epsilon)\psi|$, where ϵ and ψ are the eigenvalue and eigenstates of $\mathcal{U}$, respectively. In this way we find that for the range of volumes considered in this paper about one-tenth of the total N eigenstates is barely affected by the truncation approximation. The eigenstate presented in Fig. 8 is chosen from this one tenth.
[29] F. L. Moore, J. C. Robinson, C. F. Bharucha, Bala Sundaram, and M. G. Raizen, Phys. Rev. Lett. **75**, 4598 (1995).